Advances in Nano Research, *Vol. 15, No. 6 (2023) 495-511*
https://doi.org/10.12989/anr.2023.15.6.495

The crack propagation of fiber-reinforced self-compacting concrete containing micro-silica and nano-silica

Moosa Mazloom*, Amirhosein Abna[a], Hossein Karimpour[b] and Mohammad Akbari-Jamkarani[c]

Department of Structural and Earthquake Engineering, Faculty of Civil Engineering, Shahid Rajaee Teacher Training University, I. R. Iran

(*Received November 5, 2022, Revised August 8, 2023, Accepted August 17, 2023*)

Abstract. In this research, the impact of micro-silica, nano-silica, and polypropylene fibers on the fracture energy of self-compacting concrete was thoroughly examined. Enhancing the fracture energy is very important to increase the crack propagation resistance. The study focused on evaluating the self-compacting properties of the concrete through various tests, including J-ring, V-funnel, slump flow, and T50 tests. Additionally, the mechanical properties of the concrete, such as compressive and tensile strengths, modulus of elasticity, and fracture parameters were investigated on hardened specimens after 28 days. The results demonstrated that the incorporation of micro-silica and nano-silica not only decreased the rheological aspects of self-compacting concrete but also significantly enhanced its mechanical properties, particularly the compressive strength. On the other hand, the inclusion of polypropylene fibers had a positive impact on fracture parameters, tensile strength, and flexural strength of the specimens. Utilizing the response surface method, the relationship between micro-silica, nano-silica, and fibers was established. The optimal combination for achieving the highest compressive strength was found to be 5% micro-silica, 0.75% nano-silica, and 0.1% fibers. Furthermore, for obtaining the best mixture with superior tensile strength, flexural strength, modulus of elasticity, and fracture energy, the ideal proportion was determined as 5% micro-silica, 0.75% nano-silica, and 0.15% fibers. Compared to the control mixture, the aforementioned parameters showed significant improvements of 26.3%, 30.3%, 34.3%, and 34.3%, respectively. In order to accurately model the tensile cracking of concrete, the authors used softening curves derived from an inverse algorithm proposed by them. This method allowed for a precise and detailed analysis of the concrete under tensile stress. This study explores the effects of micro-silica, nano-silica, and polypropylene fibers on self-compacting concrete and shows their influences on the fracture energy and various mechanical properties of the concrete. The results offer valuable insights for optimizing the concrete mix to achieve desired strength and performance characteristics.

Keywords: fracture energy; micro-silica; nano-silica; self-compacting concrete; softening function

1. Introduction

Concrete is one of the most important and widely used building materials globally (Afroughsabet *et al*. 2016). Over the last decades, with the expansion of construction around the world, lots of research has been done to find new, cheaper, and widely accessible materials to reduce construction costs (Shin *et al*. 1989). One of the most notable developments in the field of concrete technology over the last two decades is self-compacting concrete (SCC) (Abna and Mazloom 2022a, Mazloom *et al*. 2021, Abna and Mazloom 2022b). This concrete is compacted by its weight and does not need any internal or external vibration. SCC can flow and fill in the molds using gravity force (Revilla-Cuesta *et al*. 2020, Skarendahl and Petersson 2000). Moreover, a high amount of cement should be used in this concrete (Topçu 2010). It is clear that high-grade cement increases the hydration temperature of the concrete, which in turn can cause new challenges like increasing the cracking in SCC. Also, the extensive use of cement has undesirable environmental and economic impacts (Topçu 2010, Mazloom *et al*. 2019a, b). To overcome these challenges, researchers have suggested using pozzolans as cement replacement materials in concrete to reduce its cement grade and solve environmental problems. Moreover, the use of pozzolans increases the compressive and tensile strength of concrete (Pachideh *et al*. 2020).

In recent studies, the relationships between different characteristics of concrete and its strength have been investigated. In some of these studies, micro-silica has been used as a substitute for cement and limestone powder has been used as filler in the mixtures. The results of one of these studies show that micro-silica increases the compressive strength and other mechanical properties of concrete (Mazloom *et al*. 2004). Pandey and Kumar (2019a) investigated the impact of rice straw ash and micro-silica on the durability properties of M40-gradee Pavement Quality Concrete (PQC). By partially substituting cement with rice straw ash and micro-silica, the concrete showed a significant reduction in water absorption and chloride ion penetration as the curing age increased and the proportion of rice straw ash and micro-silica increased. The addition of micro-silica to concrete admixed with rice straw ash resulted in the least loss of mass and compressive strength when exposed to an acidic environment, showing its effectiveness in enhancing concrete durability (Pandey and

*Corresponding author, Professor,
E-mail: Mazloom@sru.ac.ir
[a] Ph.D., E-mail: Amir.abna@gmail.com
[b] Ph.D., E-mail: karimpour.h@gmail.com
[c] M.Sc., E-mail: akbari.j143@gmail.com

ISSN: 2287-237X (Print), 2287-2388 (Online)

Kumar 2020). Moreover, they showed that the Partial substitution of Ordinary Portland Cement with 7.5% micro-silica and 5%–7.5% rice straw ash-micro silica composite resulted in the highest improvement (Pandey and Kumar, 2019b). Mazloom and his colleagues examined self-compacting concrete containing micro-silica in different experimental works (Mazloom and Ranjbar 2010, Mazloom *et al*. 2017, Afzali-Naniz and Mazloom 2018a, Afzali-Naniz and Mazloom 2018b). They showed that with the replacement of micro-silica, the mechanical properties and durability of the concrete increased. According to the results of Horszczaruk *et al*. (2013, 2014), with the addition of nano-silica, the compressive strength of concrete increased, and its permeability decreased. In another study, nano-silica increased the compressive strength of self-compacting concrete (Mazloom *et al*. 2021).

It is inevitable for concrete to develop cracks. The primary reason for this is due to the inherent weakness of concrete in tension, which is the main cause of most self-compacting concrete cracks. (Mazloom and Mirzamohammadi 2021a). Steel reinforcement can be used to solve the problem of concrete weakness in tension. Reinforcement with steel improves the strength along with the rebars' directions, while tensile forces may also occur in other directions. Using fibers is another solution for improving the tensile strength of concrete. By enhancing the isotropy of concrete cross-section, fibers reduce the fragility and brittleness of concrete (Kamal and Safan 2014). Many research projects have utilized reinforcing fibers to increase ductility, strength, and durability, as well as to prevent brittleness (Kamal and Safan 2014, Mazloom and Mirzamohammadi 2021b). Because the fibers are distributed randomly in different directions, they prevent cracks from forming between the edges of cracks in concrete by creating bridges between them (Mazloom *et al*. 2020). To increase the tensile and flexural strength of concrete, fibers must be used to provide an integrated system. Even though a variety of fibers are available, only a few of them are suitable for concrete use (Mazloom and Mirzamohammadi 2019). According to the size of the cracks, there are two types of cracks, micro, and macro. The expansion and fusion of micro-cracks make macro-cracks to be formed. Fibers must therefore be used in both micro and macro scales in concrete in order to control both types of cracks. Macro fibers are stronger than micro ones. In addition to controlling micro-cracks, they improve concrete's mechanical properties. The low mechanical properties of microfibers make them less effective in improving concrete's mechanical properties, but they do play a greater role in crack control. Furthermore, the ability of fibers to prevent crack formation depends on several factors, such as the type of fibers and their location, the adhesion between the fibers and the cement matrix, their cross-section, and their length. Regarding this, one of the most common types of concrete among modern materials is fiber-reinforced concrete (ACI 1994, Rashid Hameed 2010).

This study focuses on investigating the effects of nano-silica and micro-silica on the mechanical properties of self-compacting concrete, both individually and in combination. The scarcity of experimental and numerical studies on the synergy between these two materials prompted the research. Additionally, the study aims to enhance the fracture and mechanical characteristics of the concrete by incorporating polypropylene fibers into the mixtures. By examining fracture parameters and mechanical properties, the main objective is to analyze the behavior of fiber-reinforced self-compacting concrete containing nano-silica and micro-silica. The method in this study is the response surface method and by using this method the important relationships among the amounts of micro-silica, nano-silica, polypropylene fibers, and dependent variables (strength and fracture parameters) are shown. The response surface method (RSM) is used for optimizing the number and response of the experiments. RSM, as a widely used method in various branches of science, including medicine, physics, engineering, and chemistry, was proposed by Wilson and Box in 1951(Soares *et al*. 2002). This method is used for determining the variables affecting the response and the necessary analysis, and afterward, the mathematical relationship between the response and the set of input variables is presented (Montgomery 2017, Cho 2007). RSM can also be considered an applicable method in the field of concrete technology (Cihan *et al*. 2013).

Softening function is the primary input for modeling the fracture of concrete when the cohesive crack approach is used. In this paper, an inverse algorithm is used to find the softening curve of the concrete. This algorithm uses nonlinear finite element analysis and the damage-plasticity model. It is based on the kinematics of the beam at the late stages of loading. Using this algorithm leads to softening curves that can be used for modeling the tensile cracking of concrete precisely (Karimpour and Mazloom 2022a).

2. Experimental program

The materials used, the test methods, and the mixtures of this research are described below.

2.1 Material properties

In this research, type I-425 Portland cement with a specific weight of 3.07 g/cm^3 and the Blaine fineness of 3290 cm^2/g has been used. The micro-silica content had a specific weight of 2.21 g/cm3. The stone powder with a density of 2.68 g/cm3 has been used too. The crushed coarse aggregate had a maximum size of 12.5 mm; its specific gravity was 2.66 g/cm^3; its granulation was according to ASTM C33 (2013). River sand with a saturated surface dry density of 2.66 g/cm^3 was used too. The utilized superplasticizer was based on polycarboxylic ether. The polypropylene fibers had a length of 12 mm.

2.2 Methodology

In order to investigate the effects of polypropylene fibers, nano-silica, and micro-silica on the mechanical properties and fracture parameters of fiber-reinforced self-compacting concrete, 24 different mixtures were constructed. For this purpose, the compressive strength, tensile strength

(a) V-funnel

(b) J-ring

(c) slump

Fig. 1 Picture of fresh concrete tests

Table 1 Mix proportions of self-compacting concrete

Num	Mix ID	Cement (kg/m^3)	Coarse aggregate (kg/m^3)	Fine aggregate (kg/m^3)	Limestone powder (kg/m^3)	Micro-silica (kg/m^3)	Nano silica (kg/m^3)	Water (kg/m^3)	Superplasticizer (kg/m^3)	Fibers (kg/m^3)
1	MIX0	445.50	340	1088	272	0	0	180	4.5	0
2	M0N1P0	432.00	340	1088	272	0	4.5	180	13.5	0
3	M0N2P0	425.25	340	1088	272	0	9	180	15.75	0
4	M0N3P0	418.50	340	1088	272	0	13.5	180	18	0
5	M0N4P0	411.75	340	1088	272	0	18	180	20.25	0
6	M4N0P0	423.00	340	1088	272	18	0	180	9	0
7	M8N0P0	403.87	340	1088	272	36	0	180	10.13	0
8	M10N0P0	392.62	340	1088	272	45	0	180	12.38	0
9	M12N0P0	381.37	340	1088	272	54	0	180	14.63	0
10	M16N0P0	362.25	340	1088	272	72	0	180	15.75	0
11	M5N0.5P0	411.75	340	1088	272	22.5	2.25	180	13.5	0
12	M5N0.75P0	408.38	340	1088	272	22.5	3.375	180	15.75	0
13	M5N1P0	405.00	340	1088	272	22.5	4.5	180	18	0
14	M5N0.15P0	400.50	340	1088	272	22.5	6.75	180	20.25	0
15	M5N2P0	396.00	340	1088	272	22.5	9	180	22.5	0
16	M0N2P0.05	418.45	340	1088	272	0	9	180	18	0.455
17	M0N2P0.1	411.65	340	1088	272	0	9	180	20.25	0.91
18	M0N2P0.15	404.85	340	1088	272	0	9	180	22.5	1.365
19	M10N0P0.05	384.70	340	1088	272	45	0	180	15.75	0.455
20	M10N0P0.1	379.02	340	1088	272	45	0	180	16.88	0.91
21	M10N0P0.15	373.35	340	1088	272	45	0	180	18	1.365
22	M5N0.75P0.05	403.83	340	1088	272	22.5	3.375	180	15.75	0.455
23	M5N0.75P0.1	395.90	340	1088	272	22.5	3.375	180	19.13	0.91
24	M5N0.75P0.15	387.98	340	1088	272	22.5	3.375	180	22.5	1.365

modulus of elasticity, and fracture energy tests were performed. In this regard, for each experiment, three samples were made and tested; the average of the three results was considered the relevant parameter in the research. Due to the fact that a large part of the strength of concrete is obtained at the age of 28 days, and also in order to accurately investigate the mentioned parameters under constant conditions, all tests were performed at the age of 28 days with a constant water-to-cement ratio. The self-compacting concrete mixtures have been selected in accordance with ACI 237 (2007). Also, by modifying the mixture of self-compacting concrete, the efficiency and stability of this concrete were in the range of EFNARC standard (2002). In order to investigate the effect of polypropylene fibers on self-compacting concrete containing nano-silica and micro-silica, the following mixtures were made: mix No. 1 as a control mix without micro-silica, nano-silica, and fibers; mixtures 2 to 5 had no fibers and micro-silica and had 1%, 2%, 3%, and 4% nano-silica, respectively; mixtures 6 to 10 were free of nano-silica and fibers but had 4%, 8%, 10%, 12%, and 16% micro-silica, respectively. Also, for making binary mixes,

due to the fact that the properties of micro-silica and nano-silica are somewhat similar, at first, it was decided to use 0.05% nano-silica plus 5% or 10% micro-silica. The sample containing 5% micro-silica had higher strength and better self-compaction properties. Therefore, mixtures 11 to 15 were fiber-free and contained 5% micro-silica with 0.5%, 0.75%, 1%, 1.5%, and 2% nano-silica. It is worth presenting that the optimal percentage of nano-silica in single mixtures was 2%; therefore, mixtures 16 to 18 had 2% nano-silica plus 0.05%, 0.1%, and 0.15% of polypropylene fibers (by volume), respectively. Similarly, in mixtures containing micro-silica, the sample with 10% micro-silica was optimal, so mixtures 19 to 21 had 10% micro-silica and 0.05%, 0.1%, and 0.15% polypropylene fibers, respectively. Also, to investigate the effect of combining micro-silica, nano-silica, and polypropylene fibers, the composite samples, including 5% micro-silica and 0.75% nano-silica along with 0.05, 0.1, and 0.15% polypropylene fibers were presented in mixtures 22 to 24. The details of the mixtures with the water-to-cement ratio of 0.4 can be seen in Table 1. In the naming of the samples in Table 1, the control mix without fibers, micro-silica, and nano-silica are marked with MIX0; moreover, the ones containing micro-silica, nano-silica, and polypropylene fibers are marked with M, N, and P, respectively.

In this study, the J-ring test was performed according to ASTM C1621 (2006) to evaluate the flowability of concrete. Moreover, slump flow and V-funnel tests were performed according to EFNARC (2002). With the slump flow test, the time taken for the SCC mixture to reach the diameter of 500 mm, which indicates flowability, is measured. Also, the final diameter (D_t) of the mix, which measures filling capacity and flow rate, is measured. The j-ring test determines the ability of concrete to pass through the dense reinforcement in the formwork. The V-funnel test is designed to assess the final time for flow and passage through confined spaces without obstruction. Pictures of fresh concrete tests can be seen in Fig 1. Immediately after testing the fresh concrete to check the mechanical properties, the concrete is poured into the mold and the samples are stored at 20±2 °C in the laboratory for 24 hours. All the specimens were cured underwater for 28 days at 20 ± 2 °C. Compressive strength test was performed on 100 × 100 × 100 mm cubic specimens with a loading rate of 0.3 MPa/s according to BS 1881 part 116 (1983). To determine the elastic modulus of concrete, cylindrical specimens with a diameter of 150 and a height of 300 mm according to were used ASTM C469 (2010). A tensile strength test was performed on cylindrical specimens with a height of 300 mm and a cross-sectional diameter of 150 mm at a loading rate of 0.02 MPa/S according to BS 1881 part 117 (1983) and ASTM C496 (2017).

One of the most critical parameters affecting the crack propagation of concrete is fracture energy, which is calculated in different ways. This test is shown in Fig. 2. Based on the relationships determined by Hillerborg's proposed method, the fracture energy of the samples (GF) is obtained and has been shown in Fig. 3 and Equations 1-4 (Hillerborg 1985). the dimensions of the beams were 350×100×100 mm according to ASTM C1609 (2006), and the loading rate of this test was 0.5 mm/min. According to

Fig. 2 Sample under fracture energy test

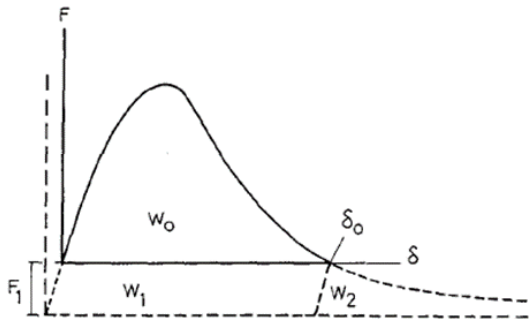

Fig. 3 Force-displacement curve in the failure method experiment (Hillerborg 1985)

ASTM C1609 (2006), the deflection equal to $\frac{l}{150}$ is the end of the test for normal concrete with fiber, this point is equal to 2 mm in this study. The test was conducted on the notched beam with crack width and height of 3 mm and 25 mm, respectively. In these equations, G_F is the fracture energy of the specimens, W_0 is the area measured below the displacement force diagram, "δ_0" is the displacement at the moment of failure, F_1 is the force due to the weight of the beam, A is the cross-sectional area of the beam (Hillerborg 1985).

$$G_F = \frac{W}{A} \ (N/mm) \quad (1)$$

$$W = W_0 + W_1 + W_2 \quad (2)$$

$$W_1 = W_2 = F_1 \delta_0 \quad (3)$$

$$W = W_0 + 2 F_1 \delta_0 \quad (4)$$

3. Numerical analysis

Due to the development of the inelastic zone at the crack tip, linear elastic fracture mechanics, LEFM, cannot be used to analyze concrete failure (Broujerdian *et al*. 2019). The fracture process zone (FPZ) is ideally composed of two zones: the bridging zone and the microcracking zone (Shi 2009).

Hillerborg *et al*. (1976) imagined a fictitious instead of a physical fracture process zone (FPZ). This assumption is the concept of cohesive zone models, suggested by Dugdale (1960) and Barenblatt (1962). The fictitious crack is

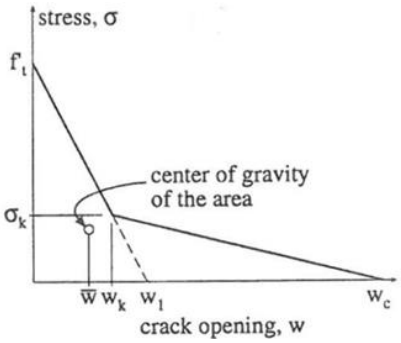

Fig. 4 Bilinear softening function (Bazant and Planas 2019)

exposed to the closure tractions, which are mainly related to bridging grains and the presence of micro-cracks. The stress at the tip of the fictitious crack is the maximum stress, which is equal to the tensile strength of concrete (f_t') (Hillerborg *et al*. 1976). These cohesive stresses correspond to the crack opening displacements, and they reduce along the fictitious crack to zero, where the concrete opening displacement reaches its critical value (W_C). At the faces of the crack where the crack opening displacement is more than the critical value, the traction-free surfaces and the real crack form (Hillerborg *et al*. 1976).

The relation between the cohesive stress acting across the crack faces and the crack opening displacement, known as softening function, describes the local behavior of the material inside the FPZ when the fracture occurs in the material. The traction separation function stipulates the transitional behavior of material from a continuous state to a discontinuous one. It clarifies how an increase in discontinuity in FPZ affects tension stresses at the crack tip (Shi 2009). Among the various functions presented for the softening behavior of concrete in tension, such as linear and exponential, the bilinear softening functions have been widely used in the literature, which is also used in this research. Karimpour and Mazloum (2019a) showed that the bilinear softening function represents the exact tensile behavior of concrete after cracking.

Fig. 4 shows the typical curve of the bilinear function. The traction separation relation of concrete has two distinct characteristics. The first is a steep slope descending section due to the rapid loss of tensile strength in the initial softening stage. The second item is a long tail that indicates the consistent stress transfer capacity of aggregates in the FPZ (Shi 2009). It can be expressed explicitly as a function of softening curve parameters. In this function (σ_k, w_k) are the coordinates of the kink point and w_c is the critical crack opening displacement. The expression of softening function in terms of bilinear softening curve parameters is:

$$\sigma = f_t'\left(1 - \frac{w}{w_1}\right) \qquad \text{For} \quad 0 \le w \le w_k$$

$$\sigma = \sigma_k\left(\frac{w - w_c}{w_k - w_c}\right) \qquad \text{For} \quad w_k \le w \le w_c \qquad (5)$$

$$\sigma = 0 \qquad \text{For} \quad w \ge w_c$$

Karimpour and Mazloom (2022a) presented a novel inverse algorithm for predicting the softening function of concrete. The motivation behind this study is that determining the softening functions is the primary and effective part of the cohesive crack model of the concrete. This algorithm is based on the kinematics of the beams at the late stages of the loading. According to the condition of equilibrium of moments, the following equation was derived:

$$p = \frac{A}{u^2} \quad \text{and} \quad A = \frac{bs}{4} G_F \overline{w} \qquad (6)$$

In the above equation, (p) is the applied load, and (u) is the deformation of the beam in the middle of its span; (b) and (s) are the width and span length of the beam, respectively. ($\overline{w}$) is the abscissa of the center of gravity of the softening function. (A) is a parameter determined by the least-square fitting of a straight line through the origin in the p-u^{-2} diagram. It should be noted that in the p-u^{-2} diagram, the first stages of the horizontal axis represent the last stages of the beam fracture. In fact, when u increases, the u^{-2} parameter decreases with the square power. The curve fitting is applied on the first stage of the curve according to the proposed model for the final loading stage.

Fig. 5 illustrates the flowchart of the proposed algorithm, explained previously, to find a softening function. The algorithm is a semi-automatic process to find the bilinear cohesive stress function of the concrete utilizing finite element software. The parameters required for this algorithm can be obtained with the help of common fracture tests. In fact, through the utilization of this algorithm in conjunction with finite element analysis, it becomes possible to accurately determine the softening curve of concrete.

4. Results and discussion

Fresh concrete tests were performed immediately after making self-compacting concrete mixes. After examining the self-compacting properties, the hardened samples were made, and their relative tests were performed. The results of the experimental part of the research are listed below.

4.1 Fresh state properties

Fresh concrete tests, including slump flow, J-ring, and V-funnel, were performed to evaluate the self-compacting properties of all samples. The results of the experiments are presented in Table 2. According to EFNARC Regulation (30) and considering Table 2, the final diameters of the slump flow for all the samples were in the range of 600-780 mm. By adding micro-silica and nano-silica to the mixes, the slump flow diameter was reduced, and it can be said that micro-silica and nano-silica decreased the rheology of the samples. With the combination of micro-silica and nano-silica, this reduction intensified and became more than the ones in the single samples. Also, according to samples 16 to 21 in Table 2, it can be said that with increasing the fibers, the time for concrete to reach the diameter of 500 mm,

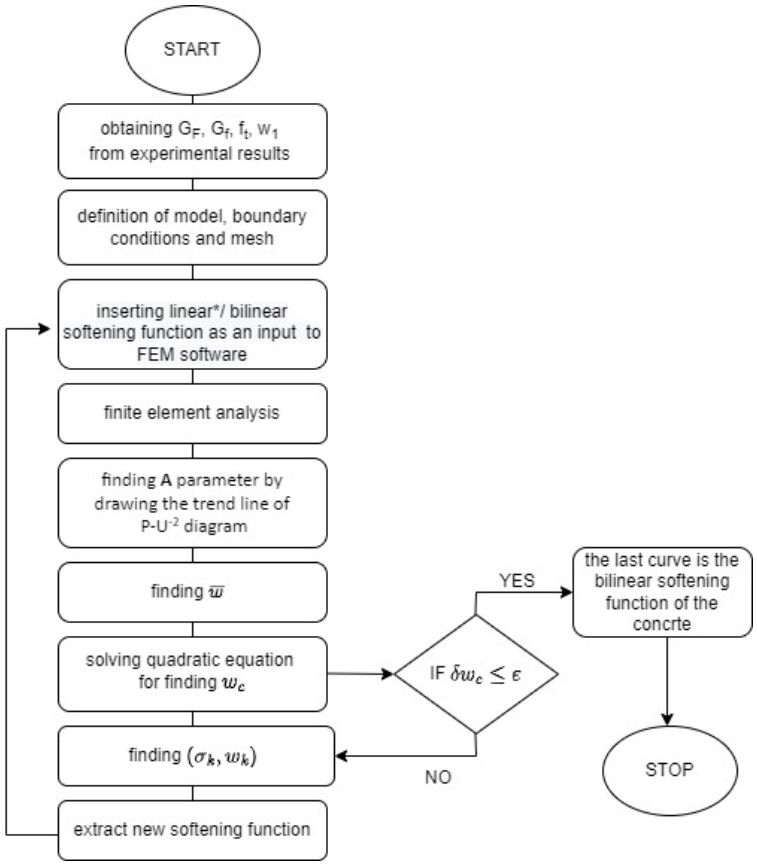

Fig. 5 Flowchart of the proposed algorithm (Karimpour and Mazloom 2022a)

which is relative to the viscosity of fresh concrete paste, increases. According to the diagram in Table 2, the mentioned times for all the samples are in the range of EFNARC regulations (EFNARC 2002). The J-ring test is based on measuring the difference in the height of concrete before and after the reinforcement grid. According to Table 2, the difference in the height for all the mixes is in the range of EFNARC regulation (EFNARC 2002). Also, the difference in the height of the J-ring test increased with improving the level of micro-silica and nano-silica, which indicates the probability of blockage in the mixes increased. The v-funnel test is designed to evaluate the final time for flow and the passage through confined spaces of the mixtures. According to Table 2, the V-funnel flow times of all samples are in the range of EFNARC regulations (EFNARC 2002). With the increase of micro-silica and nano-silica, the V-funnel flow time increased; in other words, the flow of concrete decreased. Finally, by reviewing the test results, it can be said that all the mixtures had acceptable self-compacting properties.

Compressive strength tests were performed on the samples at the age of 28 days. The results of the experiment are presented in Table 3 and Fig. 6. The MIX0 sample, which was the control mix and lacked micro-silica, nano-silica, and fibers, had a compressive strength of 44 MPa. According to Table 3, by increasing the amount of nano-silica in single samples without fibers, the compressive strength increased first and then decreased. In single samples with nano-silica, the one with 2% nano-silica had the maximum compressive strength with the strength of 52.9 MPa; the strength increased by 20% compared to the control mix. In samples containing micro-silica, with increasing replacement percentage, the compressive strength increased first and then decreased slightly. Among the samples with micro-silica, the one containing 10% micro-silica had the highest compressive strength with a strength of 51.2 MPa; the strength improved by 16% compared to the control mix. Moreover, in the samples with nano-silica and different amounts of polypropylene fibers, the one containing 2% nano-silica and 0.15% fibers had the maximum compressive strength with the strength of 53.94 MPa, which increased by 22% compared to the control mix. Among the samples without fibers and with the combination of micro-silica and nano-silica, the one containing 5% micro-silica and 1% nano-silica had the highest compressive strength. This sample with a strength of 55.19 MPa had a 25% increase in strength compared to the control mix. Among the samples with micro-silica and different amounts of fibers, the specimens containing 10% micro-silica and 0.15% of fibers had the maximum compressive strength with a strength of 52.73 MPa; the strength increased by 19% compared to the control mix. In fiber-reinforced samples, including micro-silica, nano-silica, and polypropylene fibers, the one containing 5% micro-silica, 0.75% nano-silica, and 0.1% polypropylene fibers had the highest compressive strength; also, it had had the highest compressive strength among all the samples. This mix, with a compressive strength of 57.04 MPa, was 29% better than

Table 2 Results of fresh self-compacting concrete tests

Num	Mix ID	Slump flow (mm)	T50 (s)	J-ring (mm)	V-funnel (S)
1	mix0	780	3.3	5.3	8.5
2	M0N1P0	765	3.8	5.8	9.6
3	M0N2P0	760	4	6.1	10.1
4	M0N3P0	745	4.2	6.6	11
5	M0N4P0	730	4.3	7.2	12.3
6	M4N0P0	770	3.9	5.9	8.9
7	M8N0P0	760	4.2	6.4	9.4
8	M10N0P0	755	4.5	6.8	9.8
9	M12N0P0	745	4.4	7.1	10.3
10	M16N0P0	740	4.2	7.4	11.5
11	M5N0.5P0	760	3.9	6.9	13
12	M5N0.75P0	755	4.3	7.2	14.5
13	M5N1P0	745	4.6	7.5	16
14	M5N1.5P0	740	4.7	7.8	15
15	M5N2P0	738	4.8	8	15.5
16	M0N2P0.05	750	4.9	7	14.5
17	M0N2P0.1	720	4.8	8.2	13
18	M0N2P0.15	690	5	8.5	13.5
19	M10N0P0.05	760	3.8	6.8	12.5
20	M10N0P0.1	740	4.1	7.7	15.2
21	M10N0P0.15	710	4.4	8.5	13
22	M5N0.75P0.05	680	5.2	8.8	16.5
23	M5N0.75P0.1	640	5.4	9.2	15.8
24	M5N0.75P0.15	600	5.6	9.6	17.2

the control mix. Generally speaking, according to the mentioned results, the combination of micro-silica and nano-silica in the mixtures is recommended. These materials in the concrete matrix can be used in mixes to decrease the porosity of the concrete, improve its hydration reaction in the pozzolanic reaction (production of CSH type one) and also develop its hydration activity. It is noteworthy that with the addition of nanoparticles and micro-silica to concrete, the amount of superplasticizer dosage increased.

The summary of the experimental result in this part is that with increasing micro-silica, the compressive strength increased and then decreased. With increasing nano-silica, the compressive strength improves and then reduces. By adding fibers to the samples containing micro-silica and nano-silica, the compressive strength did not change significantly. In binary samples, with the increase of micro-silica and nano-silica, in addition to increasing the costs related to the need for more superplasticizers, the compressive strength slightly decreased in some conditions. It is worth reminding that the mixture containing 5% micro-silica, 0.75% nano-silica, and 0.1% polypropylene fibers had the highest compressive strength.

According to the literature, the other researchers agree with some of the findings of this research. Mazloom *et al.* (2021) stated that nano-silica increased the compressive strength of self-compacting concrete by up to 27%. Jena and Patel (2016) investigated the effect of fibers on fiber self-compacting concrete. Their results showed that with 0.2% of glass and carbon fibers, the compressive strength increased by 15% and 35%, respectively. Jena and Mohanty (2015) also studied the effect of steel fibers on self-compacting concrete. With 1 and 2% of fibers, the compressive strength increased by 13% and 37% (Pachideh and Gholhaki 2020). Atewi *et al.* (2019) examined the effect of nano-silica on fiber self-compacting concrete. With 2% nano-silica, the compressive strength increased by 5%. Rani and Priyanka (2017) investigated the effect of PP fibers on fiber self-compacting concrete. Adding 1% of fibers increased the compressive strength by 13%. Altalabani *et al.* (2020) inspected the effect of poly-propylene fibers on self-compacting concrete, and with 0.33% of fibers, the compressive strength did not change significantly.

4.2 Splitting tensile Strength

The tensile strength test was performed on the samples at the age of 28 days. The results of the experiment are presented in Table 3 and Fig. 6. The MIX0, which was the control mix and lacked micro-silica, nano-silica, and fibers, had a tensile strength of 3.55 MPa. According to Table 3, by increasing the amount of nano-silica in single samples without fibers, the tensile strength increased first and then decreased. In single samples containing nano-silica, the one with 3% nano-silica had the maximum tensile strength, and with the strength of 3.73 MPa, it had a 5% increase in strength compared to the control mix. In specimens with micro-silica, with increasing the replacement percentage, the tensile strength increased first and then decreased slightly. Among the samples with micro-silica, the one containing 10% micro-silica had the highest tensile strength with a strength of 3.76 MPa; it had a 6% increase in strength compared to the control mix. Also, among the samples without fibers and containing the combination of micro-silica and nano-silica, the specimen containing 5% micro-silica and 1% nano-silica had the maximum tensile strength. This sample with a strength of 3.92 MPa had a 10% increase in strength compared to the control mix. Also, in samples with nano-silica and different amounts of polypropylene fibers, the one containing 2% nano-silica and 0.15% fibers had the maximum tensile strength with the strength of 4.26 MPa; this strength increased by 20% compared to the control mix. Among the samples with different amounts of fibers and micro-silica, the one containing 10% micro-silica and 0.15% fibers had the maximum tensile strength with the tensile strength of 4.5 MPa, which increased by 14% compared to the control mix. In fiber binary samples including micro-silica, nano-silica, and polypropylene fibers, the one containing 5% micro-silica, 0.75% nano-silica, and 0.15% polypropylene fibers had the highest tensile strength among all the samples. This sample with a tensile strength of 4.49 MPa improved by 26% compared to the control mix. It is worth reminding that for compressive strength, the mixture containing 5% micro-silica, 0.75% nano-silica, and 0.1% polypropylene fibers was the best. In other words, more fibers were needed to improve the tensile strength.

Table 3 Compressive and tensile strength test results

Num	Mix ID	Compressive strength (Mpa)	Percentage of compressive strength changes (%)	Tensile strength (Mpa)	Percentage of tensile strength changes (%)
1	MIX0	44(1.92)	0.0	3.55	0.00
2	M0N1P0	49.1(1.81)	11.6	3.62	1.97
3	M0N2P0	52.9(2.13)	20.2	3.69	3.94
4	M0N3P0	50.3(1.84)	14.3	3.73	5.07
5	M0N4P0	48.5(1.56)	10.2	3.64	2.54
6	M4N0P0	46.2(1.67)	5.0	3.59	1.13
7	M8N0P0	48.3(1.73)	9.8	3.67	3.38
8	M10N0P0	51.2(2.34)	16.4	3.76	5.92
9	M12N0P0	49.25(1.45)	11.9	3.69	3.94
10	M16N0P0	47.35(2.16)	7.6	3.61	1.69
11	M5N0.5P0	53.16(2.27)	20.8	3.71	4.51
12	M5N0.75P0	56.17(2.14)	27.7	3.74	5.35
13	M5N1P0	55.19(1.93)	25.4	3.92	10.42
14	M5N1.5P0	53.21(1.25)	20.9	3.83	7.89
15	M5N2P0	53.91(1.41)	22.5	3.79	6.76
16	M0N2P0.05	53.08(1.17)	20.6	4.05	14.08
17	M0N2P0.1	53.31(2.21)	21.2	4.15	16.90
18	M0N2P0.15	53.94(2.35)	22.6	4.26	20.00
19	M10N0P0.05	51.59(1.75)	17.3	3.86	98.73
20	M10N0P0.1	52.03(1.41)	18.3	3.98	12.11
21	M10N0P0.15	52.73(1.64)	19.8	4.05	14.08
22	M5N0.75P0.05	56.21(2.51)	27.8	4.33	21.97
23	M5N0.75P0.1	57.04(2.54)	29.6	4.41	24.23
24	M5N0.75P0.15	56.89(2.46)	29.3	4.49	26.48

*The numbers in the parentheses represent the standard deviation of the results (MPa)

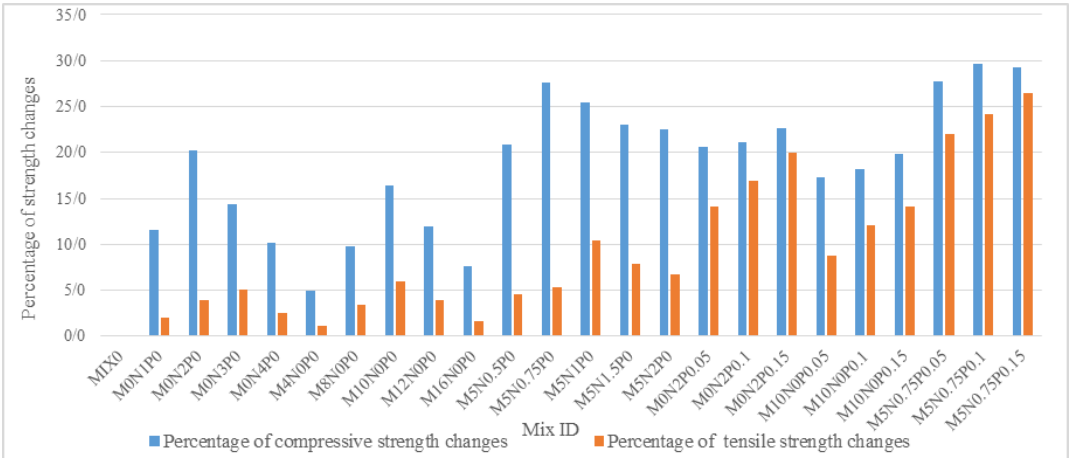

Fig. 6 Graph of percentage changes in tensile strength of fiber self-compacting concrete specimens

As micro-silica increased, the tensile strength increased and then decreased. By adding fibers to the samples containing micro-silica and nano-silica, the tensile strength, compared to the fiber-free state, changed significantly. With increasing nano-silica up to 3%, the tensile strength increased and then decreased. In binary samples, with an excessive increase of micro-silica and nano-silica, in addition to increasing the costs related to superplasticizers, the resistance parameters decreased slightly. In fact, the effect of fibers in improving tensile strength was much greater than the effect of nano-silica and micro-silica. There is some other research in this field. Jena and Patel (2016) stated that with 0.2% glass and carbon fibers, the tensile strength of fiber self-compacting concrete improved by

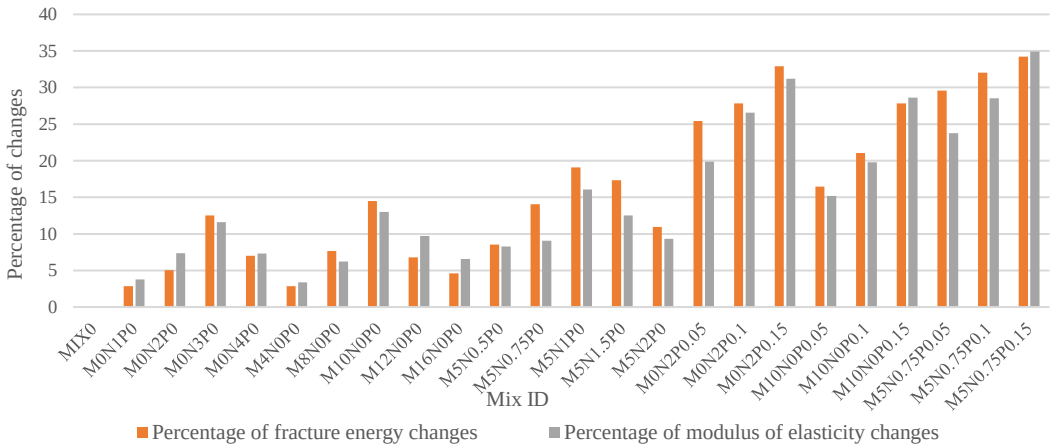

Fig. 7 Graph of percentage changes in modulus of elasticity and fracture energy of self-compacting concrete specimens

Table 4 Fracture energy and modulus of elasticity of the specimens

Num	Mix ID	Fracture energy (N/mm)	Percentage of fracture energy changes (%)	Modulus of elasticity (GPa)	Percentage of elastic modulus changes (%)
1	MIX0	4.56	0	25.27	0
2	M0N1P0	4.69	2.9	26.22	3.8
3	M0N2P0	4.79	5.0	27.13	7.4
4	M0N3P0	5.13	12.5	28.2	11.6
5	M0N4P0	4.88	7.0	27.12	7.3
6	M4N0P0	4.69	2.9	26.12	3.4
7	M8N0P0	4.91	7.7	26.84	6.2
8	M10N0P0	5.22	14.5	28.55	13.0
9	M12N0P0	4.87	6.8	27.73	9.7
10	M16N0P0	4.77	4.6	26.93	6.6
11	M5N0.5P0	4.95	8.6	27.36	8.3
12	M5N0.75P0	5.2	14.0	27.56	9.1
13	M5N1P0	5.43	19.1	29.33	16.1
14	M5N1.5P0	5.35	17.3	28.43	12.5
15	M5N2P0	5.06	11.0	27.63	9.3
16	M0N2P0.05	5.72	25.4	30.29	19.9
17	M0N2P0.1	5.83	27.9	31.98	26.6
18	M0N2P0.15	6.06	32.9	33.16	31.2
19	M10N0P0.05	5.31	16.4	29.11	15.2
20	M10N0P0.1	5.52	21.1	30.27	19.8
21	M10N0P0.15	5.83	27.9	32.5	28.6
22	M5N0.75P0.05	5.91	29.6	31.28	23.8
23	M5N0.75P0.1	6.02	32.0	32.48	28.5
24	M5N0.75P0.15	6.12	34.2	34.1	34.9

10% and 20%, respectively. Jena and Mohanty (Jena and Mohanty 2015) reported an increase in the tensile strength of fiber self-compacting concrete by 23% when adding 2% steel fibers. Atewi *et al*. (2019) investigated the effect of nano-silica on fiber-reinforced self-compacting concrete and reported a 2% improvement in tensile strength with 2% nano-silica. Çelik and Bingöl (2020) also examined fiber self-compacting concrete. They noted that by adding 0.3% of the fibers, the tensile strength increased by 11.6%.

4.3 Fracture properties

The other specifications of the specimens, including fracture energy and modulus of elasticity, are presented in Table 4. Also, the graph of the percentage changes of the samples compared to the control mix is shown in Fig. 7. Regarding the information in Table 4, the fracture energy of the MIX0 sample was 4.56 N/mm; this sample did not include micro-silica, nano-silica, and fibers. By increasing

the percentage of micro-silica replacement in the samples containing micro-silica, the fracture energy first increased and then decreased slightly.

Among them, the sample with 10% micro-silica had the maximum fracture energy of 5.22 N/mm, which was 14.5% better than the control mix. As the amount of nano-silica in the fiber-free samples increased, the fracture energy increased first and then decreased.

In fiber-free samples containing nano-silica, the maximum fracture energy of the sample with 3% nano-silica was 5.13 N/mm; it was 12.5% higher than the control mix. Also, among the binary samples without fibers, the one containing 5% micro-silica and 1% nano-silica had the maximum fracture energy with a value of 5.43 N/mm. This sample improved by 19% compared to the control mix. In samples with nano-silica and different amounts of polypropylene fibers, the sample containing 2% nano-silica and 0.15% fibers had the maximum fracture energy of 6.06 N/mm, which was 32% better than the control mix. The specimen containing 10% micro-silica and 0.15% fibers had the highest fracture energy, with a value of 5.83 N/mm among the samples containing micro-silica. This sample was 27% better than the control mix. Also, among the fiber samples with micro-silica and nano-silica, the sample containing 5% micro-silica, 0.75% nano-silica, and 0.15% polypropylene fibers had the highest fracture energy, equal to 6.12 N/mm. It was 34% better than the control mix. It is worth noting that this mixture had the best tensile strength as well.

According to Table 4 and Fig. 7, it can be seen that the modulus of elasticity behaved similarly to the fracture energy. In other words, with increasing the fracture energy, the modulus of elasticity increased too. Of course, the amounts of increase or decrease in the modulus of elasticity were different from those of the fracture energy. In the study for single samples, the maximum modulus of elasticity was for the one with 10% micro-silica and also 3% nano-silica. The modulus of elasticity of these samples increased by 13% and 11% compared to the control mix, respectively. Moreover, the fiber-free binary sample with 1% nano-silica and 5% micro-silica had the maximum modulus of elasticity. The samples with 0.15% fibers and 10% micro-silica or 2% nano-silica had the maximum modulus of elasticity which increased by 28% and 31%, respectively, compared to the control mix. The best binary fiber samples had 5% micro-silica, 0.15% fibers, and 0.75% nano-silica. This sample with a modulus of elasticity of 34.1 GPa was 34% better than the control mix. It is clear that the above mix had the best tensile strength and fracture energy too. Only for compressive strength, the mixture containing 5% micro-silica, 0.75% nano-silica, and 0.1% polypropylene fibers was the best.

Atewi *et al.* (2019) investigated fiber self-compacting concrete containing nano-silica. They found with a 2% increase in nano-silica, the fracture energy increased by 17%. Altalabani *et al.* (2020) examined the effect of poly-propylene fibers on self-compacting lightweight concrete. They said by adding 0.33% of fibers, the modulus of elasticity improved by 4.6% compared to the control mix. It is worth reminding that by adding fibers to the samples, the fracture energy changed considerably compared to the fiber-free states. Al-Hadithi *et al.* (2019) inspected the self-compacting fiber-reinforced concrete. According to this research, the best sample had 1.5% of fibers; the elastic modulus of this sample increased by 20% compared to the control mix .In recent years, many researchers have studied the fracture and mechanical properties of different cementitious composites with and without fibers (Bolander *et al.* 2008, Karamloo and Mazloom 2018, Mazloom and Salehi 2018, Li *et al.* 2020, Afzali-Naniz and Mazloom 2019b, Nikbin *et al.* 2016, Prakasam *et al.* 2020, Salehi and Mazloom 2018, Salehi and Mazloom 2019a, Salehi and Mazloom 2019b). Generally speaking, they agree with the trend of the results presented in this paper.

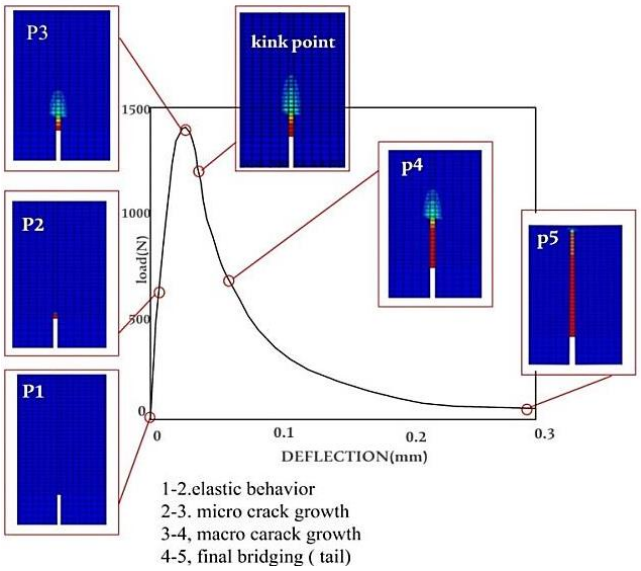

Fig. 8 Load-deflection curve of the concrete beam

4.4 Analytical results

The coordinates of the bilinear curves obtained from the proposed algorithm for different mixtures are given in Table 5. The N parameter is the number of iterations made to achieve convergence in this table.

Fig. 8 shows the different zones of concrete load-displacement curves. The curve initially behaves linearly from zero to p_2. After p_2, the initial micro-cracks that existed before loading in the cement paste aggregate interface begin to grow. This non-elastic phase continues until it reaches the ultimate loading capacity of the specimen, known as the peak load (p_3). After (p_3), the specimen is damaged and fractured due to the micro-crack coalescence, and the curve shows a downward trend (p_4 & p_5). As the curve descends, the micro-cracks become unstable, and localized cracking occurs over a narrow area of micro-cracks termed as fracture process zone (FPZ).

From the obtained results, it is clear that the critical crack opening displacement (w_c) of fiber-reinforced concrete is much larger than that of plain concrete. This is because the fibers prevent the coalescence of microcracks and prevent their propagation, delaying the formation of macrocracks (Karimpour and Mazloom 2022b).

Table 5 Characteristics of softening models obtained from the proposed algorithm

Num	Mix ID	A parameter	w_1 (*mm*)	w_c (*mm*)	w_k (*mm*)
1	MIX0	7.85E+04	1. 541	4.624	1.028
2	M0N1P0	8.11E+04	1.555	4.664	1.036
3	M0N2P0	8.30E+04	1.558	4.673	1.038
4	M0N3P0	9.20E+04	1.650	4.951	1.100
5	M0N4P0	8.62E+04	1.609	4.826	1.073
6	M4N0P0	8.16E+04	1.568	4.703	1.045
7	M8N0P0	8.66E+04	1.605	4.816	1.070
8	M10N0P0	9.41E+04	1.666	4.998	1.111
9	M12N0P0	8.52E+04	1.584	4.751	1.056
10	M16N0P0	8.35E+04	1.586	4.757	1.057
11	M5N0.5P0	8.72E+04	1.601	4.803	1.067
12	M5N0.75P0	9.39E+04	1.668	5.005	1.112
13	M5N1P0	9.78E+04	1.662	4.987	1.108
14	M5N1.5P0	9.68E+04	1.676	5.029	1.117
15	M5N2P0	8.92E+04	1.602	4.806	1.068
16	M0N2P0.05	1.33E+05	1.412	7.062	1.059
17	M0N2P0.1	1.35E+05	1.405	7.024	1.054
18	M0N2P0.15	1.42E+05	1.423	7.113	1.067
19	M10N0P0.05	1.21E+05	1.376	6.878	1.032
20	M10N0P0.1	1.27E+05	1.387	6.935	1.040
21	M10N0P0.15	1.38E+05	1.440	7.198	1.080
22	M5N0.75P0.05	1.34E+05	1.365	6.824	1.024
23	M5N0.75P0.1	1.37E+05	1.365	6.825	1.024
24	M5N0.75P0.15	1.39E+05	1.363	6.815	1.022

N* represents the number of itterartions.

4.5 Response Surface Methodology (RSM)

Response Surface Methodology (RSM) was used to analyze the experimental data in this study. The dependent variables of the analysis include compressive strength, tensile strength, modulus of elasticity, and fracture energy. Also, independent variables were micro-silica, nano-silica, and fiber percentages. The results were obtained by Design Expert 7.0 modeling software and the response surface relationships method. In fact, the response's dependent variables in terms of independent ones were obtained using response surface methodology.

It should be noted that in this study, all the experiments were performed first, and then the relationships between dependent and independent variables were investigated. To determine the relevant relationships in this method, the analysis of variance was performed with a significance level of α=0.1, and the results were evaluated. Due to the value of α = 0.1, the P values are not accepted for sentences larger than 0.1; therefore, in the next step, the mentioned sentences were removed from the answer function, and analysis of variance was performed again. The p values were re-examined, and finally, the final models were presented, which were described in detail below. The results of the analysis of variance are presented in Tables 6 and 7 according to the final approved model. In addition, the final relationships among the variables are described in Eqs. 7-10, where "*A*" represents the amount of micro-silica, "*B*" represents the amount of nano-silica, and "*C*" represents the amount of polypropylene fibers; all the three parameters were examined in terms of kg/m^3. Moreover, the three-dimensional response surfaces are shown in Fig. 9(a-e).

$$\text{Compressive strength} = 57.1971-4.6944B2+3.1732A3+2.1107B3+1.9935C3 \quad (7)$$

$$\text{Tensile strength} = 6.0329-0.5958C2+1.4004ABC-0.7290A2B+0.9461A2C-0.7080AB2-0.5226AC2+0.8377B2C-0.4450BC2-0.2126C3 \quad (8)$$

$$\text{Modulus of elasticity} = 30.7168-2.3514C2+7.7658ABC-3.7017A2B+4.9935A2C-3.3662AB2-2.0062AC2+3.9148B2C-2.8676BC2-1.5524A3 \quad (9)$$

$$\text{Fracture energy} = 5.6146+0.3519A2C+0.1420BC2+0.4129C3 \quad (10)$$

According to Tables 6, and 7 and the graphs in Fig. (9-a), the effect of the variables on the compressive strength was investigated and the relationship between them is

Table 6 ANOVA for Cube Reaction Levels Decrease Level of Analysis of Variance (for Mechanical Parameters)

Type of experiment	Factor	Sum of Squares	df	Mean Square	F-Value	p-value	R-Squared
R1- Compressive strength	Source Model	219.7275	4	54.9319	18.2553	< 0.0001	0.9603
	B^2	141.9158	1	141.9158	47.1625	< 0.0001	
	A^3	47.3124	1	47.3124	15.7232	0.0008	
	B^3	77.5644	1	77.5644	25.7767	< 0.0001	
	C^3	45.4539	1	45.4539	15.1055	0.0010	
	Residual	57.1726	19	3.0091			
	Cor Total	276.9001	23				
R2- Tensile strength	Source Model	1.6880	8	0.2110	54.5471	< 0.0001	0.9872
	B	0.1107	1	0.1107	28.6199	< 0.0001	
	B^2	0.3433	1	0.3433	88.7508	< 0.0001	
	ABC	0.0817	1	0.0817	21.1308	0.0003	
	A^2C	0.0267	1	0.0267	6.8972	0.0191	
	AB^2	0.2237	1	0.2237	57.8303	< 0.0001	
	AC^2	0.0546	1	0.0546	14.1076	0.0019	
	BC^2	0.0272	1	0.0272	7.0212	0.0182	
	C^3	0.4797	1	0.4797	124.0185	< 0.0001	
	Residual	0.0580	15	0.0039			
	Cor Total	1.7460	23				
R3- modulus of elasticity	Source Model	136.1144	9	15.1238	48.4592	< 0.0001	0.9842
	C^2	5.0855	1	5.0855	16.2946	0.0012	
	ABC	25.5561	1	25.5561	81.8859	< 0.0001	
	A^2B	9.3763	1	9.3763	30.0432	< 0.0001	
	A^2C	43.1044	1	43.1044	138.1135	< 0.0001	
	AB^2	17.4078	1	17.4078	55.7774	< 0.0001	
	AC^2	1.6117	1	1.6117	5.1641	0.0393	
	B^2C	44.0764	1	44.0764	141.2279	< 0.0001	
	BC^2	6.2961	1	6.2961	20.1737	0.0005	
	A^3	3.5211	1	3.5211	11.2822	0.0047	
	Residual	4.3693	14	0.3121			
	Cor Total	140.4837	23				

Table 7 ANOVA for Cube Reaction Levels Decrease Level of Analysis of Variance (for fractures Parameters)

Type of experiment	factor	Sum of Squares	df	Mean Square	F-Value	p-value	R-Squared
R5- Fracture energy	Source Model	4.5126	3	1.5042	30.0979	< 0.0001	0.9744
	A^2C	0.4058	1	0.4058	8.1189	0.0099	
	BC^2	0.2071	1	0.2071	4.1437	0.0553	
	C^3	1.1544	1	1.1544	23.0980	0.0001	
	Residual	0.9995	20	0.0500			
	Cor Total	5.5122	23				

specified in Eq. 7. According to Table 6 and Fig. 9, R^2 = 0.96, which indicates the suitability of the proposed model. Also, according to Tables 6, and 7, the F-values for B^2 and A^3 are larger than the others (P-value<0.05), which indicates the great effect of micro-silica and nano-silica on the compressive strength. The F value of B^2 is also greater than the F-value of A^3, which according to experimental results, shows that the effect of nano-silica on compressive strength is much greater than that of micro-silica. For this reason, the consumption of nano-silica was much lower than micro-silica. Also, according to the graph in Fig. 9-a, the effect of fibers on compressive strength is very low. This low impact may be due to the fact that the fibers reduce the adhesion between the cement and the aggregate.

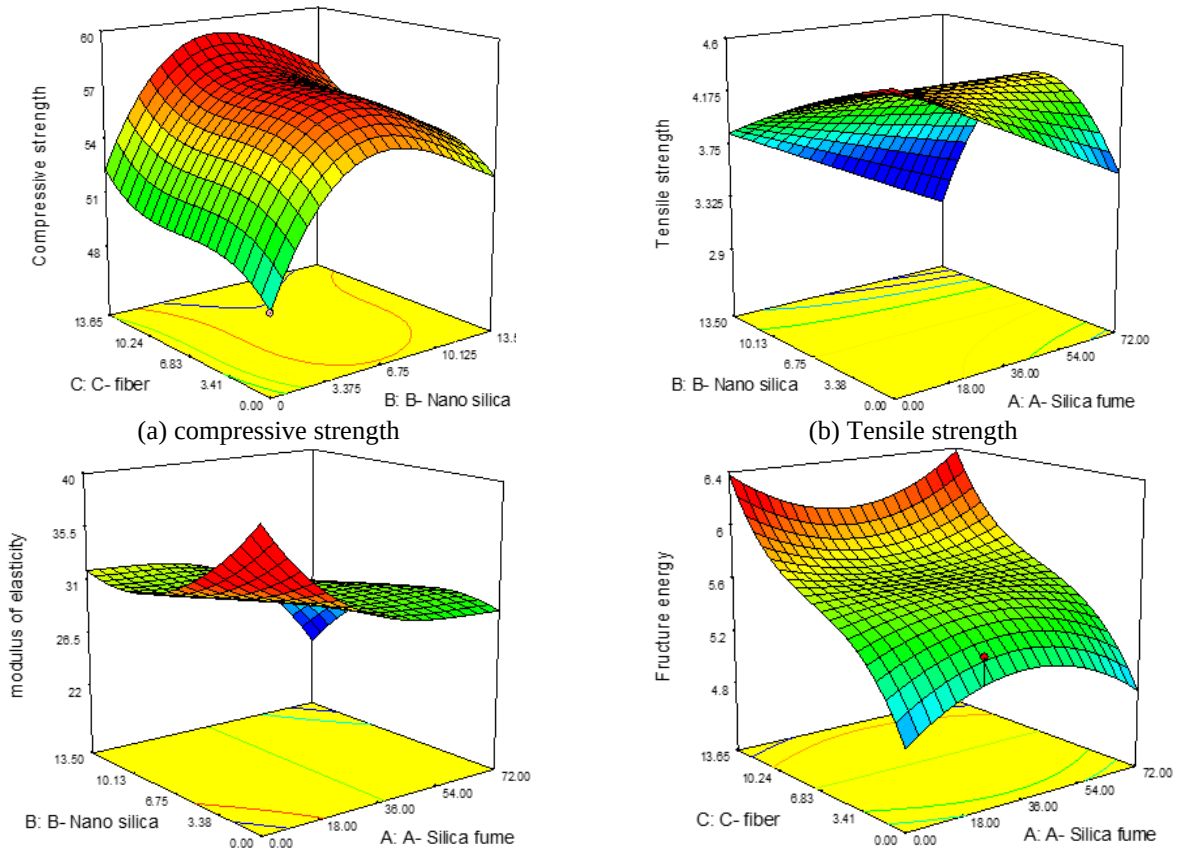

(a) compressive strength (b) Tensile strength

(c) Modulus of elasticity (d) fracture energy

Fig. 9 Three-dimensional plots in RSM design

Despite the fibers, nano-silica has a great effect on compressive strength.

The relationship between variables on tensile strength was also presented in Equation 8. For tensile strength, R^2 = 0.98, which indicates the suitability of the proposed model. The F-value, according to Tables 6, and 7 for expression B^2 and especially C^3 are larger than the others, which shows the very high effect of fibers and the relatively moderate effect of nano-silica on tensile strength (P-value<0.05). According to the graph in Fig. 9-b, the effect of micro-silica and nano-silica on tensile strength is high. However, according to Fig. 9, with increasing the amount of micro-silica and nano-silica, the tensile strength has slightly decreased, which is due to the high consumption of superplasticizers.

In reviewing the results of the analysis of variance for modulus of elasticity, it is obvious that R^2 = 0.98, which confirms the proposed models. The relationship between the variables on these parameters was presented in Equation 9, respectively. For modulus of elasticity, F-values were maximum for A^2C and B^2C expressions, respectively, indicating the high effect of fibers on these two parameters (P-value<0.05). According to Fig. 9-c, the effect of micro-silica and nano-silica on the modulus of elasticity is high. Of course, their effect is much less than the effect of fibers. The combination of high amounts of micro-silica and nano-silica, due to the use of the superplasticizer, reduces the effect of these parameters.

Finally, the effect of variables on failure energy was investigated, and the relationship between variables is presented in Equation 10. According to Tables 6, 7, and Fig. 9-d, the proposed model was appropriate because R2 = 0.97. Also, the F-value for the expression C3 is larger than the rest, which indicates the great effect of fibers on the fracture energy (P-value<0.05). Based on the information in Fig. 9-d, micro-silica has a negligible effect on the fracture energy. In addition, fibers have a high impact on fracture energy; this is due to the fact that fibers limit the spread of cracks.

4.5 Microstructure of specimens

Fig. 10 shows the electron microscope images of the samples at the age of 28 days. Sample (a) of this figure is free of any nano and microparticles (control mix). It is clear that the control sample is quite porous. Images (b), (c), and (d) of Fig. 10 show the ones containing nano-silica, micro-silica, and binary samples containing micro-silica plus nano-silica, respectively. It is observable that nano-silica and micro-silica had positive effects on lowering the porosity of the specimens. In fact, they act as fillers due to the fineness of their particles; moreover, they have pozzolanic properties. The samples (b) and (c) are denser, and the cavities and discontinuities between the particles are less.

Also, the structures of these samples are very homogeneous. In other words, their microstructures are better

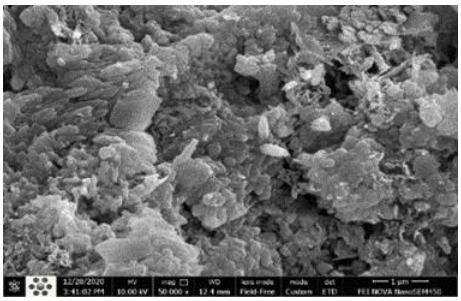
(a) Control mix

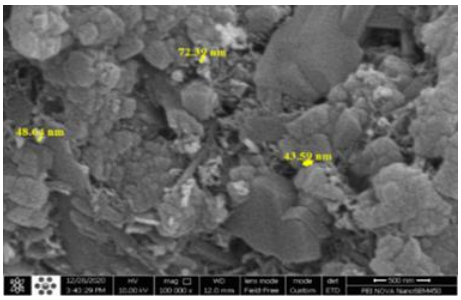
(b) M0N2P0

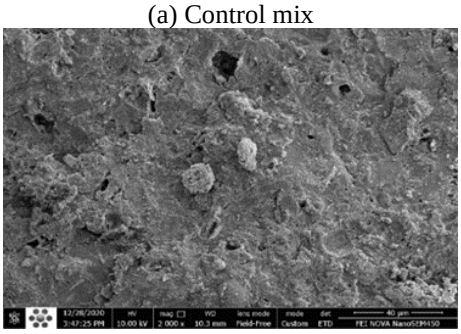
(c)M10N0P0

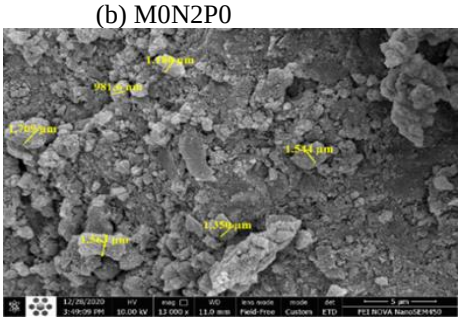
(d) M5N1P0

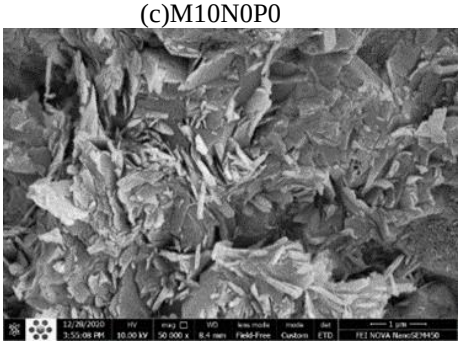
(e)M0N2P0.15

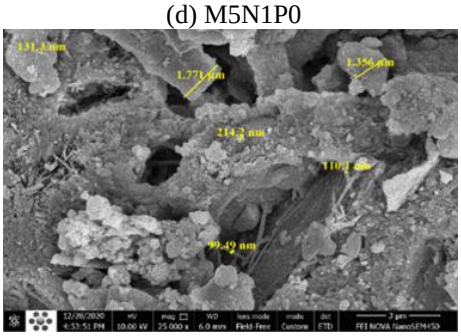
(f) M10N0P0.15

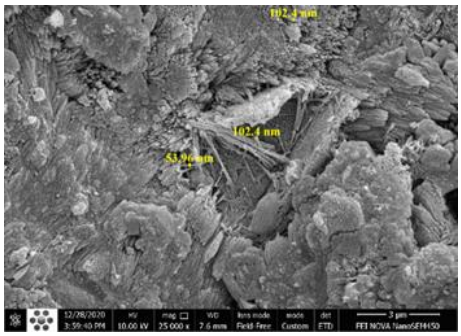
(g) M5N0.75P0.15

Fig. 10 Scanning electronic microscope (SEM) images of the samples

than the control mix. Also, the microstructure of the concrete with nano-silica is denser than the one containing micro-silica. According to image (d), the binary mixture containing micro-silica and nano-silica had the densest microstructure. It is clear that the amounts of cavities and voids are less in this concrete. Therefore, its mechanical properties and fracture energy have improved. The images (e, f) are for the samples containing micro-silica plus fibers and nano-silica plus fibers, respectively. It is observable that the distribution of polypropylene fibers is very homo-geneous and random, which leads to an increase in strength parameters, especially the tensile strength of the samples. It is worth reminding that all specimens had the same water-to-cement ratio; moreover, they have been fabricated and tested under similar conditions. Therefore, less porosity and capillary were considered as a sign of increasing the degree of hydration using micro-silica and nano-silica (Image g).

5. Conclusions

This study focuses on the utilization of pozzolans in fiber-reinforced self-compacting concrete with the aim of enhancing fracture energy, which is crucial for resisting crack propagation. The main objectives of this research were to reduce cement consumption, enhance tensile

strength, improve mechanical properties, and optimize fracture parameters in self-compacting concrete. The investigation examined the effects of three materials (micro-silica, nano-silica, and polypropylene fibers) on the mechanical properties and fracture energy of fiber-reinforced self-compacting concrete. These materials were studied both independently and in various combinations, resulting in a total of 24 different concrete mixtures. To analyze the influence of these materials, the study employed response surface methodology to establish significant relationships between the variables under investigation. The findings of the research are as follows:

• In single additive mixtures, with the addition of micro-silica or nano-silica, the compressive strength, tensile strength, and fracture energy of self-compacting concrete were first increased and then decreased. In binary mixes containing micro-silica and nano-silica, compressive strength, tensile strength, and fracture energy increased at least about 27.7%, 10%, and 19.1 compared to the single ones.

• In all fiber samples, with increasing the amount of fibers up to 0.15%, the amount of compressive and tensile strengths increased. However, the addition of polypropylene fibers reduced the rheology of the mixes. Micro-silica and nano-silica had the same effect on fresh concrete. However, in this study, all samples could obtain suitable self-compacting conditions. In other words, it is possible to produce self-compacting concrete containing micro-silica, nano-silica, and polypropylene fibers simultaneously.

• The main positive effect of micro-silica and nano-silica was to improve the mechanical properties, especially the compressive strength of the specimens. The main constructive impacts of fibers were to increase the tensile strength and fracture energy of the samples. With the combination of micro-silica, nano-silica, and polypropylene fibers, compressive strength, tensile strength, and fracture energy increased by 29.6%, 26.4% and 34% respectively, compared to the control mix.

• Of all the binary samples with fibers, one had the highest compressive strength, which had 5% micro-silica, 0.75% nano-silica, and 0.1% polypropylene fibers. This specimen had a compressive strength of 57.04 MPa, which was 29.6% higher than the control mix. Additionally, the most efficient binary mix for tensile strength and fracture energy contained 5% micro-silica, 0.75% nano-silica, and 0.15% polypropylene fibers. This sample's tensile strength, modulus of elasticity, and fracture energy were equal to 4.49 MPa, 34.1 GPa, and 6.12 N/mm, respectively, which enhanced by 26%, 34.9% and 34.2%, respectively, in comparison to the control mix.

• According to SEM images, micro-silica and nano-silica have caused homogeneity and relative density of the samples. Also, these materials have increased the compressive strength of self-compacting concrete by reducing its cavities. According to electron microscope images, polypropylene fibers could control the micro-cracks because of random distribution and bridging between the cracks; therefore, polypropylene fibers could increase the tensile strength and fracture energy of the specimens.

• The softening curves of the mixes are obtained from an inverse algorithm proposed by the authors. It is demonstrated that the algorithm, which is based on nonlinear finite element analysis, can determine the softening curves of plain and fiber-reinforced concrete. The softening curves are critical input properties of concrete for accurate modeling of tensile cracks. Moreover, it has been shown that the critical crack opening displacement of fiber-reinforced concrete is larger than that of plain concrete due to the bridging effect of fibers.

• As shown in the analysis of variance (ANOVA), micro-silica and nano-silica had a significant impact on the compressive strength of self-compacting concrete. It should be considered that the impact of nano-silica was higher than that of micro-silica. Polypropylene fibers had a great influence on the fracture energy and tensile strength but they did not have a considerable effect on the compressive strength. However, by mixing the fibers with micro-silica and nano-silica, they had a higher impact on the compressive strength.

Acknowledgments

This work was supported by Shahid Rajaee Teacher Training University under grant number 4951.

References

Abna, A. and Mazloom, M. (2022a), "Flexural properties of fiber reinforced concrete containing silica fume and nano-silica", *Mater. Lett.*, **316**, 132003. https://doi.org/10.1016/j.matlet.2022.13200.

Abna, A. and Mazloom, M. (2022b), "The effects of micro-silica and nano-silica on the workability and mechanical properties of self-compacting concrete containing polypropylene fibers", *Amirkabir J. Civil Eng.*, **54**(3), 1101-1118. https://doi.org/10.22060/CEEJ.2021.19252.7115.

ACI 237 (2007), *Self-Consolidating Concrete*, American Concrete Institute.

ACI Committee 544 Report (1994), *Design Consideration for SFRC, ACI structural journal*, 563-530.

Afroughsabet, V., Biolzi, L. and Ozbakkaloglu, T (2016), "High-performance fiber-reinforced concrete: A review", *J. Mater. Sci.*, **51**(14), 6517-6551. https://doi.org/10.1007/s10853-016-9917-4.

Afzali-Naniz, O. and Mazloom, M. (2018), "Effects of colloidal nano-silica on fresh and hardened properties of self-compacting lightweight concrete", *J. Build. Eng.*, **20**, 400-410. https://doi.org/10.1016/j.jobe.2018.08.014.

Afzali-Naniz, O. and Mazloom, M. (2019a), "Assessment of the influence of micro- and nano-silica on the behavior of self-compacting lightweight concrete using full factorial design", *Asian J. Civil Eng.*, **20**, 57-70. https://doi.org/10.1007/s42107-018-0088-2.

Afzali-Naniz, O. and Mazloom, M. (2019b), "Fracture behavior of self-compacting semi-lightweight concrete containing nano-silica", *Adv. Struct. Eng.*, **22**(10), 2264-2277. https://doi: 10.1177/1369433219837426.

Al-Hadithi, A.I., Noaman, A.T. and Mosleh, W.K. (2019), "Mechanical properties and impact behavior of PET fiber reinforced self-compacting concrete (SCC)", *Compos. Struct.*, **224**, 111021. https://doi.org/10.1016/j.conbuildmat.2019.08.029

Altalabani, D., Bzeni, K. and Linsel, S. (2020), "Mechanical

properties and load-deflection relationship of polypropylene fiber reinforced self-compacting lightweight concrete", *Const. Build. Mater.*, **252**, 119084 https://doi.org/10.1016/j.conbuildmat.2020.119084

ASTM C1609/M-05 (2006), *Standard Test Method for Flexural Performance of Fiber Reinforced Concrete (using Beam with Third-point loading)*, ASTM International, West Conshohocken Pennsylvania.

ASTM C1621 (2006), *Standard Test Method for Passing Ability of Self-Consolidating Concrete by J-Ring*. ASTM International.

ASTM C496/C496M (2017), *Standard Test Method for Splitting Tensile Strength of Cylindrical Concrete Specimens*, ASTM International.

ASTM C469/C469M (2010), *Standard Test Method for Static Modulus of Elasticity and Poisson's Ratio of Concrete in Compression*, ASTM International.

ASTM C33 (2013), *Standard specification for concrete aggregates*. *Philadelphia*, ASTM International.

Bolander, E., Choi, S. and Duddukuri, S.R. (2008), "Fracture of fiber-reinforced cement composites: effects of fiber dispersion", *Int. J. Fract.*, **154**, 73-86. https://doi.org/10.1007/s10704-008-9269-4.

Barenblatt, G.I. (1962), "The mathematical theory of equilibrium cracks in brittle fracture", *Adv. Appl. Mech.*, **7**, 55-129. https://doi.org/10.1016/S0065-2156(08)70121-2.

Broujerdian, V., Karimpour, H. and Alavikia, S. (2019), "Predicting the shear behavior of reinforced concrete beams using nonlinear fracture mechanics", *Int. J. Civil Eng.*, **17**(5), 597-605. https://doi.org/10.1007/s40999-018-0336-6.

BS 1881: Part 116 (1983), *Method for Determination of Compressive Strength of Concrete Cubes*, British Standards.

BS 1881: Part 117 (1983), *Method for Determination of Tensile Splitting Strength*, British Standards.

Çelik, Z. and Bingöl, A.F. (2020), "Fracture properties and impact resistance of self-compacting fiber reinforced concrete (SCFRC)", *Mater. Struct.*, **53**(3), 1-16. https://doi.org/10.1617/s11527-020-01487-8

Cho, T. (2007), "Prediction of cyclic freeze–thaw damage in concrete structures based on response surface method", *Constr. Build. Mater.*, **21**(12), 2031-2040. https://doi.org/10.1016/j.conbuildmat.2007.04.018

Cihan, M.T., Güner, A. and Yüzer, N. (2013), "Response surfaces for compressive strength of concrete", *Constr. Build. Mater.*, **40**, 763-774. https://doi.org/10.1016/j.conbuildmat.2012.11.048

Dugdale, D.S. (1960), "Yielding of steel sheets containing slits", *J. Mech. Phys. Solids*, **8**(2), 100-104. https://doi.org/10.1016/0022-5096(60)90013-2

Hillerborg, A., Modéer, M. and Petersson, P.E. (1976), "Analysis of crack formation and crack growth in concrete by means of fracture mechanics and finite elements", *Cement Concr. Res.*, **6**(6), 773-781. https://doi.org/10.1016/0008-8846(76)90007-7.

EFNARC, (2002), *Specifications and Guidelines for Self-Compacting Concrete*, ISBN0 953973344.

Hillerborg, A. (1985), "The theoretical basis of a method to determine the fracture energy GF of concrete", *Mater. Struct.*, **18**(4), 291-296. https://doi.org/10.1007/BF02472919

Horszczaruk, E., Mijowska, E., Cendrowski, K. and Sikora, P. (2014), "Influence of the new method of nano-silica addition on the mechanical properties of cement mortars", *Cement, Wapno, Beton*, **5**, 308-316.

Horszczaruk, E., Mijowska, E., Cendrowski, K., Mijowska, S. and Sikora, P. (2013), "The influence of nano-silica with different morphology on the mechanical properties of cement mortars", *Cement, Wapno, Beton*, **18/80**(1), 24-32.

Jena, B. and Mohanty, B.B. (2015), "Study on the mechanical properties and fracture behavior of chopped steel fiber reinforced self compacting concrete", *Int. Res. J. Eng. Technol.*, **4**(12), 166-170.

Jena, B. and Patel, A. (2016), "Study on the mechanical properties and microstructure of chopped carbon fiber reinforced self compacting concrete", *Technology*, **7**(3), 223-232.

Kamal, M.M., Safan, M.A., Etman, Z.A. and Kasem, B.M. (2014), "Mechanical properties of self-compacted fiber concrete mixes", *HBRC J.*, **10**(1), 25-34. https://doi.org/10.1016/j.hbrcj.2013.05.012

Karamloo, M. and Mazloom, M. (2018), "An efficient algorithm for scaling problem of notched beam specimens with various notch-to-depth ratios", *Comput. Concr*, **22**(1), 39-51. http://doi.org/10.12989/cac.2018.22.1.039.

Karimpour, H. and Mazloom, M. (2022a)," Determining a novel softening function for modeling the fracture of concrete", *Adv. Mater. Res.*, **11**(4), 351. https://doi.org/10.12989/amr.2022.11.4.351

Karimpour, H. and Mazloom, M. (2022b), "Pseudo-strain hardening and mechanical properties of green cementitious composites containing polypropylene fibers", *Struct. Eng. Mech.*, **81**(5), 575-589. https://doi.org/10.12989/sem.2022.81.5.575.

Li, J., Wan, C., Zhang, X. and Niu, J. (2020), "Fracture property of polypropylene fiber-reinforced lightweight concrete at high temperatures", *Magazine Concr. Res.*, **72**(22), 1147-1154. https://doi.org/10.1680/jmacr.17.00432

Mazloom, M. and Mirzamohammadi, S. (2019), "Thermal effects on the mechanical properties of cement mortars reinforced with aramid, glass, basalt, and polypropylene fibers", *Adv. Mater. Res.*, **8**(2), 137-154. http://doi.org/10.12989/amr.2019.8.2.137.

Mazloom, M. and Mirzamohammadi, S. (2021a), "Fracture of fiber-reinforced cementitious composites after exposure to elevated temperatures", *Mag. Concr. Res.*, **73**(14), 701-713. https://doi.org/10.1680/jmacr.19.00401.

Mazloom, M. and Mirzamohammadi, S. (2021b), "Computing the fracture energy of fiber reinforced cementitious composites using response surface methodology", *Adv. Comput. Des*, **6**(3), 225-239. http://dx.doi.org/10.12989/acd.2021.6.3.225.

Mazloom, M., Pourhaji, P. and Afzali-Naniz, O. (2021), "Effects of halloysite nanotube, nano-silica and micro-silica on rheology, hardened properties and fracture energy of SCLC", *Struct. Eng. Mech.*, **80**(1), 91-101. https://doi.org/10.12989/SEM.2021.80.1.091.

Mazloom, M. and Ranjbar, A. (2010), "Relation between the workability and strength of self-compacting concrete", *Proceedings of the 35th Conference on Our World in Concrete & Structures*, Singapore, 315-322.

Mazloom, M., Karimpanah, H. and Karamloo, M. (2020), "Fracture behavior of monotype and hybrid fiber reinforced self-compacting concrete at different temperatures", *Adv. Concr. Constr.*, **9**(4), 375-386. https://doi.org/10.12989/acc.2020.9.4.375.

Mazloom, M., Pourhaji, P., Shahveisi, M. and Jafari, S.H. (2019a), "Studying the Park-Ang damage index of reinforced concrete structures based on equivalent sinusoidal waves", *Struct. Eng. Mech.*, **72**(1), 845-859. http://doi.org/10.12989/sem.2019.72.1.083.

Mazloom, M., Mehrvand, M., Pourhaji, P. and Savaripour, A. (2019b), "Studying the effects of CFRP and GFRP sheets on the strengthening of self-compacting RC girders", *Struct. Monit. Maint.*, **6**(1), 47-66. https://doi.org/10.12989/smm.2019.6.1.047.

Mazloom, M., Ramezanianpour, A.A. and Brooks, J.J. (2004), "Effect of micro-silica on mechanical properties of high-strength concrete", *Cement Concr. Compos.*, **26**(4), 347-357. https://doi.org/10.1016/S0958-9465(03)00017-9.

Mazloom, M. and Salehi, H. (2018), "The relationship between fracture toughness and compressive strength of self-compacting

lightweight concrete", *IOP Conference Series Mater. Sci. Eng.*, **431**(6). https://doi.org/10.1088/1757-899X/431/6/062007.
Montgomery, C. (2017), *Design and Analysis of Experiments*, John Wiley & Sons.
Nikbin, I.M., Davoodi, M.R., Fallahnejad, H. and Rahimi, S. (2016), "Influence of mineral powder content on the fracture behaviors and ductility of self-compacting concrete", *J. Mater. Civ. Eng.*, **28**(3). https://doi.org/10.1061/(ASCE)MT.1943-5533.0001404.
Pachideh, G. and Gholhaki, M. (2020), "Assessment of post-heat behavior of cement mortar incorporating micro-silica and granulated blast-furnace slag", *J. Struct. Fire Eng.*, **11**(2), 221-246. https://doi.org/10.1108/JSFE-11-2018-0038
Pachideh, G., Gholhaki, M. and Ketabdari, H. (2020), "Effect of pozzolanic wastes on mechanical properties, durability and microstructure of the cementitious mortars", *J. Build. Eng.*, **29**, 101178. https://doi.org/10.1016/j.jobe.2020.101178
Pandey, A. and Kumar, B. (2019a), "Evaluation of water absorption and chloride ion penetration of rice straw ash and micro silica admixed pavement quality concrete", *Heliyon*, **5**(8). https://doi.org/10.1016/j.heliyon.2019.e02256.
Pandey, A. and Kumar, B. (2019b), "Effects of rice straw ash and micro silica on mechanical properties of pavement quality concrete", *J. Build. Eng.*, **26**, 100889. https://doi.org/10.1016/j.jobe.2019.100889.
Pandey, A. and Kumar, B. (2020), "Investigation on the effects of acidic environment and accelerated carbonation on concrete admixed with rice straw ash and micro silica", *J. Build. Eng.*, **29**, 101125. https://doi.org/10.1016/j.jobe.2019.101125.
Prakasam, G., Murthy, A.R. and Saffiq Rehman, M. (2020), "Mechanical, durability and fracture properties of nano-modified FA/GGBS geopolymer mortar", *Magaz. Concr. Res.*, **72**(4), 207-216. https://doi.org/10.1680/jmacr.18.00059
Rani, B.S. and Priyanka, N. (2017), "Self-Compacting Concrete using Polypropylene Fibers", *Int. J. Res. Stud. Sci., Eng. Technol.*, **4**(1), 16-19.
Rashid Hameed, M. (2010), "Contribution of metallic fibers on the performance of reinforced concrete structures for the seismic application", Thesis for Ph.D., University of Toulouse, France.
Revilla-Cuesta, V., Skaf, M., Chica, J.A., Fuente-Alonso, J.A. and Ortega-López, V. (2020), "Thermal deformability of recycled self-compacting concrete under cyclical temperature variations", *Mater. Lett.*, **278**, 128417. https://doi.org/10.1016/j.matlet.2020.128417
Salehi, H. and Mazloom, M. (2018), "Effect of magnetic-field intensity on fracture behaviors of self-compacting lightweight concrete", *Mag. Concr. Res.*, **71**(13), 665-679. https://doi.org/10.1680/jmacr.17.00418.
Salehi, H. and Mazloom, M. (2019a), "Opposite effects of ground granulated blast-furnace slag and micro-silica on the fracture behavior of self-compacting lightweight concrete", *Constr. Build. Mater*, **222**, 622-632. https://doi.org/10.1016/j.conbuildmat.2019.06.183.
Salehi, H. and Mazloom, M. (2019b), "An experimental investigation on fracture parameters and brittleness of self-compacting lightweight concrete containing magnetic field treated water", *Arch. Civ. Mech. Eng.*, **19**, 803-819. https://doi.org/10.1016/j.acme.2018.10.008.
Shi, Z. (2009), *Crack Analysis in Structural Concrete: Theory and Applications*, Butterworth-Heinemann.
Shin, S.W., Ghosh, S.K. and Moreno, J. (1989), "Flexural ductility of ultra-high-strength concrete members", *Struct. J.*, **86**(4), 394-400. https://doi.org/10.1016/j.conbuildmat.2019.08.029
Skarendahl, Å. and Petersson, Ö. (2000), Report 23: Self-Compacting Concrete–State-of-the-Art Report of Rilem Technical Committee 174-SCC, RILEM publications.
Soares, C., Mohamed, A., Venturini, W.S. and Lemaire, M. (2002), "Reliability analysis of nonlinear reinforced concrete frames using the response surface method", *Reliabil. Eng. Syst. Safe.*, **75**(1), 1-16. https://doi.org/10.1016/S0951-8320(01)00043-6
Topçu, İ.B. and Uygunoğlu, T. (2010), "Effect of aggregate type on properties of hardened self-consolidating lightweight concrete (SCLC)", *Constr. Build. Mater.*, **24**(7), 1286-1295. https://doi.org/10.1016/j.conbuildmat.2009.12.007

CC